NASA TECHNICAL NOTE

NASA TN D-7802

NASA TN D-7802

EFFECTS OF VARIOUS EXPERIMENTAL PARAMETERS ON ERRORS IN TRIANGULATION SOLUTION OF ELONGATED OBJECT IN SPACE

Sheila Ann T. Long

Langley Research Center

Hampton, Va. 23665

NATIONAL AERONAUTICS AND SPACE ADMINISTRATION • WASHINGTON, D. C. • FEBRUARY 1975

1. Report No.	2. Government Accession No.	3. Recipient's Catalog No.
NASA TN D-7802		

4. Title and Subtitle	5. Report Date
EFFECTS OF VARIOUS EXPERIMENTAL PARAMETERS ON ERRORS IN TRIANGULATION SOLUTION OF ELONGATED OBJECT IN SPACE	February 1975
	6. Performing Organization Code
7. Author(s)	8. Performing Organization Report No.
Sheila Ann T. Long	L-9803
	10. Work Unit No.
9. Performing Organization Name and Address	879-11-36-01
NASA Langley Research Center Hampton, Va. 23665	11. Contract or Grant No.
	13. Type of Report and Period Covered
12. Sponsoring Agency Name and Address	Technical Note
National Aeronautics and Space Administration Washington, D.C. 20546	14. Sponsoring Agency Code

15. Supplementary Notes

16. Abstract

The effects of various experimental parameters on the displacement errors in the triangulation solution of an elongated object in space due to pointing uncertainties in the lines of sight have been determined. These parameters were the number and location of observation stations, the object's location in latitude and longitude, and the spacing of the input data points on the azimuth-elevation image traces. The displacement errors due to uncertainties in the coordinates of a moving station have been determined as functions of the number and location of the stations. The effects of incorporating the input data from additional cameras at one of the stations were also investigated.

17. Key Words (Suggested by Author(s))	18. Distribution Statement
Triangulation Barium ion cloud Errors Curved object	Unclassified – Unlimited STAR Category 30

19. Security Classif. (of this report)	20. Security Classif. (of this page)	21. No. of Pages	22. Price*
Unclassified	Unclassified	28	$3.75

*For sale by the National Technical Information Service, Springfield, Virginia 22151

EFFECTS OF VARIOUS EXPERIMENTAL PARAMETERS ON ERRORS IN TRIANGULATION SOLUTION OF ELONGATED OBJECT IN SPACE

By Sheila Ann T. Long
Langley Research Center

SUMMARY

The effects of various experimental parameters on the displacement errors in the triangulation solution of an elongated object in space due to pointing uncertainties in the lines of sight have been determined. These parameters were the number and location of the observation stations, the object's location in latitude and longitude, and the spacing of the input data points on the azimuth-elevation image traces. The displacement errors due to uncertainties in the coordinates of a moving station have been determined as functions of the number and location of the stations. The effects of incorporating the input data from additional cameras at one of the stations were also investigated.

For complex multistation triangulation problems such as this, the displacement errors were shown to depend on the combination of observation stations, the input uncertainties, and the weighting scheme for the data. The formulas, procedures, and many numerical results of this paper may be used for any experiment which requires precision triangulation of elongated objects in space.

INTRODUCTION

The present studies were made in direct support of the National Aeronautics and Space Administration/Max Planck Institute for Extraterrestrial Physics Barium Ion Cloud (BIC) Experiment. The objectives of this experiment were to determine, in the proximity of the release, the shape and orientation of the magnetic field line from the cloud elongation and the strength and direction of the electric field from the cloud drift. References 1 and 2 discuss the experiment and the results that were obtained.

In the present paper the effects of various experimental parameters on pointing displacement errors in the triangulation solution of an elongated object in space due to pointing uncertainties in the lines of sight are determined. These parameters are the number and location of observation stations, the object's location in latitude and in longitude, and the spacing of input data points on the azimuth-elevation image traces.

The station displacement errors due to uncertainties in the coordinates of a moving station as functions of the number and location of stations are determined. The effects of incorporating the input data from additional cameras at one of the stations are investigated.

These results were used in planning the BIC experiment and in establishing the data-reduction procedure for the experiment. For example, they were used in selecting the observation stations and in formulating the "go" launch criteria which would be used in the event of unfavorable weather or equipment malfunction at one or more of the stations. Because of the long delay time $\left(\text{about } 3\frac{1}{2} \text{ hr}\right)$ between launch and release, there was still no guarantee that, once the payload had been launched, the weather would remain favorable and the equipment would continue to function during the observation period. Hence, these results were also used in estimating the loss of triangulation accuracy caused by loss of data from one or more stations during the observation period. These results were also used in establishing the number of input data points to be read from the azimuth-elevation image traces and in deciding whether to incorporate the input data from additional cameras at one of the stations.

The coordinates of the release point and the shape and orientation of the elongated object in space that are given in the present paper are realistic to the BIC experiment. The observation stations are the ones investigated for the experiment. The triangulation method used (described in ref. 3) is the one adopted for the experiment. However, even if an elongated object with different characteristics is used, together with different stations and a different triangulation method (such as the ones described in refs. 4 to 6), the numerical results given in the present paper can still provide insights into the effects of the various experimental parameters on the displacement errors in the triangulation solution. These numerical results are helpful, since analytical expressions for such complex multistation triangulation problems do not exist. Reference 7 also gives numerical results which are helpful to such problems.

The formulas for computing the displacement errors in the triangulation solution of an elongated object in space are derived in reference 8. These formulas, along with the formulas and the procedures that are developed in the present paper, may be used to plan any experiment which requires the precision triangulation of elongated objects in space.

SYMBOLS

e_E, e_N moving-station coordinate uncertainties directed easterly and northerly, km

e_n^{μ} pointing uncertainty along normal to azimuth-elevation image trace from station μ at nth point on trace, deg

$\Delta\lambda_M, \Delta\phi_M$ uncertainties in east longitude and geocentric latitude of moving station corresponding to uncertainties e_E and e_N, deg

ρ_M geocentric radius of moving station, km

σ standard deviation

ϕ_M geocentric latitude of moving station, deg

PRELIMINARY INFORMATION

Barium Ion Cloud

To familiarize the reader with the particular elongated object in space which provided the basis for the present study, the barium ion cloud is briefly described. The reader is referred to references 1 and 2 for more complete discussions of the cloud.

On September 20, 1971, at 23^h31^m u.t., a payload of neutral barium was launched in a four-stage Scout rocket from Wallops Island, Virginia. Approximately 1.7 kg of neutral barium were released on September 21 at $3^h4^m52^s$ u.t. at 6.926^o geodetic latitude, -74.395^o east longitude, and 31 482-km altitude.

The neutral barium rapidly became ionized by incoming solar radiation. The charged particles attached themselves to a magnetic field line, spiraled along it, and thus formed an elongated cloud along the direction of the magnetic field line.

Against a dark-sky background the barium ion cloud could be photographed from various observation stations. Figure 1 is a photograph of the cloud as seen from Mt. Hopkins, Arizona. All triangulation cameras at the different stations were synchronized in time. The photographs of the elongated cloud were compared with appropriate star charts, and the respective star configurations were matched. Thus, the right ascension and declination coordinates (which were transformed to azimuth and elevation coordinates) of selected points along the center line of the elongated cloud image were obtained.

By triangulating on the azimuth-elevation input data thus obtained from the various observation stations (with the triangulation method described in ref. 3), the position as a function of the time and, hence, the drift velocity of the barium ion cloud were determined. From the drift velocity, the strength and direction of the electric field were computed in reference 2.

Observation Stations

The observation stations investigated in the present paper were selected only after careful study. The relative locations were of major importance because long base lines

were required for triangulation. The weather conditions during the launch-window periods for the BIC experiment were also of major importance, since clear skies were required to obtain the photographic data. Table I lists the stations and their respective coordinates.

The two prime observation stations which had to be clear for the "go" launch criteria were Cerro Tololo, Chile, and Mt. Hopkins, Arizona. Additional stations, included to improve the triangulation accuracy, were Arequipa, Peru, and White Sands, New Mexico.

The NASA aircraft was the Convair 990, a high-altitude research aircraft equipped as an airborne optical observatory. A north-eastern observation station was desired to improve the triangulation accuracy; and since the east coast is frequently obscured by cloud cover, it was decided to use a high-altitude aircraft. In the present study, the aircraft was assumed to fly at an altitude of 10.7 km (35 000 ft) in the vicinity of Wallops Island, Virginia. (Because of an engine malfunction, the aircraft was used as a ground-based station during the actual experiment.)

Triangulation Method

The triangulation method employed is described in reference 3. This method applies to an object in space having no identifiable structural features and having a width that is very small compared with its length, so that it can be regarded as a curved line. The method uses as its input data the azimuth and elevation angles of photographic image points of the elongated object from several observation stations.

Input Uncertainties

In the present paper two types of input uncertainties are considered. The first type refers to pointing uncertainties in the lines of sight from the observation stations to points on the elongated object in space. The second type refers to uncertainties in the coordinates of the moving station. The pointing uncertainties and the moving-station coordinate uncertainties are propagated by the triangulation into pointing displacement errors and station displacement errors, respectively.

For the BIC experiment every effort was made to minimize input uncertainties and, thereby, maximize the triangulation precision. For example, the oblateness of Earth and the proper motions of the stars were taken into account. However, because of the very high altitude of the BIC release and the high elevation angles from the observation stations, the effects of atmospheric refraction were negligible.

Pointing uncertainties.- The coordinates of the ground-based cameras, were assumed to be precisely known. Slight uncertainties were present, however, since primary survey points at the different observation stations were located by different survey sources. Relative to the primary survey point for a given station, one corner of

each instrumentation pad was located, and coordinates of the cameras were then taken as the coordinates of their respective instrumentation-pad corners. The maximum uncertainties in the camera coordinates due to these two sources of error were estimated to be about 50 m in horizontal distance and about 2.5 m in altitude, which were negligible for this experiment.

A significant source of input uncertainty from the data acquisition system was the systematic distortion due to nonlinearity of the image intensifiers used in conjunction with the cameras. Calibration corrections (described in ref. 9) were made for this distortion. After the calibrations, however, there still remained an estimated input uncertainty of about 0.0025° in the center line of the cloud image.

A significant source of input uncertainty from the data reduction procedure was uncertainty in the image coordinates measured from the photographs of the barium ion cloud. This was due to inability to define precisely the center line of the cloud image. An exercise to determine the consistency of measurements of the center line was conducted by W. F. Landon at Wallops Flight Center, Wallops Island, Virginia. By using one of the better quality photographs, it was determined that there existed a standard deviation of 0.0032° in the center line of the cloud image due to this source of uncertainty. At other epochs, the cloud images were fuzzier and, hence, the standard deviations were greater.

The input uncertainty denoted by e_n^{μ} is along the normal to the azimuth-elevation image trace from station μ at the nth point on the trace. On the basis of the sources of input uncertainties previously discussed, the upper bound value of e_n^{μ} is assumed to be 0.01°. Hence, this value is used for computations in the present paper.

Moving-station coordinate uncertainties.- The second type of input uncertainty considered in the present paper refers to uncertainties in the coordinates of the moving observation station. The coordinates of the aircraft camera would not be so accurately known as the coordinates of the ground-based cameras. Because of its chosen flight path, the aircraft would be out of range of existing radar stations during a significant portion of the flight. During this time the aircraft's inertial navigation system would be the sole means for determining the aircraft's horizontal coordinates. This system would accumulate a 3σ error, in the aircraft's horizontal position, of 1.6 km for each hour of flight time. The error in altitude would be negligible.

The input uncertainties denoted by e_N and e_E are directed northerly and easterly, respectively. On the basis of the source of input uncertainty previously discussed, the upper bound value of both e_N and e_E is assumed to be $\sqrt{3}$ km. Hence, this value is used for computations in the present paper. The corresponding uncertainties in the geocentric latitude and the east longitude (denoted by $\Delta\phi_M$ and $\Delta\lambda_M$, respectively) of the moving station are

$$\Delta\phi_M = \frac{e_N}{\rho_M} = 0.0155^o \tag{1}$$

$$\Delta\lambda_M = \frac{e_E}{\rho_M \cos \phi_M} = 0.0197^o \tag{2}$$

where ϕ_M and ρ_M are the geocentric latitude and the geocentric radius of the moving station, respectively.

Procedure for Computing Displacement Errors

After determining what input uncertainties exist, it is important to determine how these uncertainties are propagated by the triangulation into displacement errors in the solution of the elongated object in space. For example, in the BIC experiment it was necessary to know the accuracy of the calculated position of the barium ion cloud in order to evaluate the final results of the electric-field calculations of reference 2.

In reference 8, methods for calculating displacement errors in the triangulation solution of an elongated object in space due to input errors in the azimuth-elevation image traces are derived. These errors are functions of the position along and errors in the solution curve. The component displacement errors are east-west, north-south, and radial displacement errors. The total displacement error is the square root of the sum of the squares of these components.

Since the barium ion cloud for the experiment elongated along a magnetic field line, the field line through the BIC nominal release point was chosen to be the nominal curve (required for application of the formulas derived in ref. 8). The nominal release point was selected for this preliminary work; its coordinates were 9.23^o geodetic latitude, -75.00^o east longitude, and 31 600-km altitude. The model for the international geomagnetic reference field was obtained from reference 10.

Then, the coordinates of the points along the nominal curve (in geocentric latitude, longitude, and range coordinates) are transformed to azimuth, elevation, and range coordinates from the observation stations of interest (listed in table I). These transformed coordinates constitute the input data for the triangulation program discussed in reference 3. Applying the formulas in reference 8, in conjunction with the pointing uncertainties e_n^μ, produces the pointing displacement errors. Applying these formulas, in conjunction with the moving-station coordinate uncertainties e_N and e_E, gives the station displacement errors. In the following section the pointing and the station displacement errors are given as functions of various experimental parameters.

RESULTS

Effect of Number and Location of Stations on Pointing Displacement Errors

Various cases composed of different combinations of the five observation stations listed in table I are investigated. These cases are all possible combinations of from two to five observation stations with the constraint that the two prime stations, Mt. Hopkins and Cerro Tololo, are always included. An additional case composed of Mt. Hopkins and Cerro Tololo with an additional camera at Mt. Hopkins is also investigated. (Additional cameras were placed at the stations for backup purposes.) These different station combinations are the following nine cases:

Case 1	Cerro Tololo Mt. Hopkins Arequipa NASA aircraft White Sands
Case 2	Cerro Tololo Mt. Hopkins Arequipa White Sands
Case 3	Cerro Tololo Mt. Hopkins Arequipa NASA aircraft
Case 4	Cerro Tololo Mt. Hopkins NASA aircraft White Sands
Case 5	Cerro Tololo Mt. Hopkins White Sands
Case 6	Cerro Tololo Mt. Hopkins NASA aircraft
Case 7	Cerro Tololo Mt. Hopkins Arequipa
Case 8	Cerro Tololo Mt. Hopkins Mt. Hopkins
Case 9	Cerro Tololo Mt. Hopkins

Figures 2 to 5 are plots of the east-west, north-south, radial, and total pointing displacement errors as functions of the geocentric latitude for the nine cases of

observation-station combinations. As the number of stations decreases, the errors increase. For example, for case 1 (five stations) at a latitude of 9^{o} (which is close to the nominal), east-west, north-south, radial, and total errors are about 3, 24, 33, and 41 km, respectively. For case 9 (two stations) at a latitude of 9^{o}, the corresponding errors are about 5, 35, 47, and 58 km.

It is also seen from figures 2 to 5 that case 8 (two prime stations with an additional camera at Mt. Hopkins) produces smaller pointing displacement errors than case 9. For example, at the geocentric latitude of 9^{o}, the east-west, north-south, radial, and total errors are reduced to about 5, 30, 40, and 51 km, respectively.

Effect of Object's Location in Latitude on Pointing Displacement Errors

In the proximity of the BIC nominal release point, which is close to the prime geomagnetic meridian, a magnetic field line is approximately constant in longitude. Hence, the barium ion cloud elongated in latitude and altitude.

For purposes of comparing the east-west, north-south, radial, and total pointing displacement errors, the results for case 1 (five stations) are plotted together in figure 6 over the range of geocentric latitude from -9^{o} to 28^{o}. The east-west error remains practically constant over this range of latitude and is the smallest error component. From the BIC nominal release latitude of 9.23^{o}, the north-south error decreases toward both ends and is the greatest component throughout the latitudinal region from 16^{o} to 28^{o}. The radial and total errors increase toward the lower latitude end and decrease toward the higher latitude end. Throughout the latitudinal region from -9^{o} to 15^{o}, the radial error is the greatest component.

Effect of Object's Location in Longitude on Pointing Displacement Errors

For this investigation it is convenient to examine the effect of varying release points in east longitude. For the BIC nominal release latitude and altitude and over the range of longitude from -49^{o} to -119^{o}, the elevation angles from each of the five observation stations are approximately 20^{o} or greater (a requirement imposed by the experiment). Six different release points which have the BIC nominal release latitude and altitude and longitudes of -49^{o}, -63^{o}, -77^{o}, -91^{o}, -105^{o}, and -119^{o} are investigated. Input data for the elongated object in space from the five stations are azimuth and elevation points from each of Earth's magnetic field lines corresponding to these release points.

Figures 7 to 10 are plots of the east-west, north-south, radial, and total pointing displacement errors as functions of the geocentric latitude, for case 1 (five stations) for

release points varying in east longitude. These plots were examined to determine the impact on the triangulation accuracy of the expected east-west drift from the BIC nominal release longitude of -75.00°. Errors increase as the object drifts eastward into the longitudinal regions of -63° and -49°, and errors decrease as the object drifts westward into the region of -91°. As the object drifts farther westward into the regions of -105° and -119°, errors increase or decrease depending on the object's latitude.

Effect of Spacing of Input Data Points on Pointing Displacement Errors

In establishing the data-reduction procedure for the BIC experiment, it was necessary to determine the impact on the triangulation accuracy of the spacing of the input data points on the azimuth-elevation image traces. Six different values of the spacing are investigated; these values are 0.28°, 0.56°, 1.12°, 2.24°, 4.48°, and 8.96°.

Table II gives for case 1 (five stations) the average (over the geocentric latitude) east-west, north-south, radial, and total pointing displacement errors for these six different values of the spacing. It is seen that little is to be gained from using spacings smaller than about 2.24°.

Station Displacement Errors

For determining the station displacement errors, only observation-station combinations which include the aircraft are investigated. These are cases 1, 3, 4, and 6.

Figure 11 is a plot of the east-west station displacement error as a function of the geocentric latitude for these cases. As the number of stations decreases, the east-west error increases.

Figures 12 to 14 are plots of the north-south, radial, and total station displacement errors as functions of the geocentric latitude for cases 1, 3, 4, and 6. For these errors case 3 (four stations) yields smaller errors than case 1 (five stations) and case 6 (three stations) yields smaller errors than case 4 (four stations). For example, for the latitude of 9°, cases 3, 1, 6, and 4 produce total errors of about 21, 26, 40, and 45 km, respectively. These results might, at first, appear to be contrary to the results from reference 11 and from figures 2 to 5 and 11, which all indicate that displacement errors decrease as the number of stations increases. However, from the previous listing of station combinations, it is seen that case 1 is equal to case 3 with White Sands added and case 4 is equal to case 6 with White Sands added. From table I it is seen that the coordinates of White Sands are close to those of Mt. Hopkins. Hence, case 1 is approximately equal to case 3 with an additional camera at Mt. Hopkins and also case 4 is

approximately equal to case 6 with an additional camera at Mt. Hopkins. The effect on the station displacement errors of incorporating the input data from an additional camera at Mt. Hopkins is investigated next.

Table III gives the station displacement errors for the five-station case as functions of the geocentric latitude. Table IV gives the errors for the five-station case with incorporation of the input data from an additional camera at Mt. Hopkins. The east-west error has remained the same; but the north-south, radial, and total errors have increased slightly. Table V gives the errors for the five-station case with the incorporation of the input data from two additional cameras at Mt. Hopkins. Again the east-west error has remained the same, but the north-south, radial, and total errors have increased further. Hence, with respect to station displacement errors, the addition of White Sands is equivalent to the incorporation of input data from an additional camera at Mt. Hopkins.

In this analysis the incorporation of the input data from an additional camera at a particular observation station is equivalent to giving a heavier weighting to the data from that one station. Hence, the displacement errors, which depend not only on the combination of stations and on the input errors but also on the weighting scheme for the data, could no more be expected to decrease than to increase when adding White Sands to a given station combination.

CONCLUDING REMARKS

First, the effects of various experimental parameters on the pointing displacement errors in the triangulation solution of an elongated object in space due to pointing uncertainties of 0.01° in the lines of sight were determined. For the observation stations investigated, the errors increase as the number of stations decreases. At a geocentric latitude of 9°, the five-station and two-station cases yield total errors of about 41 and 58 km, respectively. For the five-station case the radial component is the greatest component of the total error vector throughout the latitudinal region from -9° to 15°. The north-south component is the greatest component in the latitudinal region from 16° to 28°. The total error increases (from the barium ion cloud (BIC) nominal release latitude of 9.23°) toward lower latitudes and decreases toward higher latitudes. For the five-station case the errors increase as the object drifts eastward (from the BIC nominal release longitude of -75.00°) into the longitudinal regions of -63° and -49°. The errors decrease as the object drifts westward into the region of -91° longitude. As the object drifts farther westward into the regions of -105° and -119° longitude, the errors increase or decrease depending on the object's latitude. For the five-station case the average errors show that little is to be gained from using spacings (of the input data points on the azimuth-elevation image traces) smaller than about 2.24°.

Second, the station displacement errors due to uncertainties of $\sqrt{3}$ km in the coordinates of a moving observation station were determined. At a geocentric latitude of 9°, the errors increase from 21 to 26 km when White Sands is added to a four-station case, and the errors increase from 40 to 45 km when White Sands is added to a three-station case. Furthermore, the incorporation of the input data from one or two additional cameras at Mt. Hopkins in the five-station case produces increased total station displacement errors. However, the incorporation of the input data from an additional camera at Mt. Hopkins in the two-station case yields decreased total pointing displacement errors. Hence, for such complex multistation triangulation problems, the displacement errors depend on the combination of observation stations, the input uncertainties, and the weighting scheme for the data.

Even though the present studies were made in direct support of the BIC experiment, they are of general interest. The formulas and the procedures that are developed, plus many of the numerical results, may be used to plan any experiment which requires precision triangulation of elongated objects in space.

Langley Research Center,
National Aeronautics and Space Administration,
Hampton, Va., December 16, 1974.

REFERENCES

1. Brence, W. A.; Carr, R. E.; Gerlach, J. C.; and Neuss, Hans: NASA/Max Planck Institute Barium Ion Cloud Project. J. Geophys. Res., vol. 78, no. 25, Sept. 1, 1973, pp. 5726-5731.

2. Adamson, D.; Fricke, C. L.; Long, S. A. T.; Landon, W. F.; and Ridge, D. L.: Preliminary Analysis of NASA Optical Data Obtained in Barium Ion Cloud Experiment of September 21, 1971. J. Geophys. Res., vol. 78, no. 25, Sept. 1, 1973, pp. 5769-5784.

3. Fricke, Clifford L.: Triangulation of Multistation Camera Data To Locate a Curved Line in Space. NASA TN D-7538, 1974.

4. Justus, C. G.; Edwards, H. D.; and Fuller, R. N.: Analysis Techniques for Determining Mass Motions in the Upper Atmosphere From Chemical Releases. AFCRL-64-187, U.S. Air Force, Jan. 1964. (Available from DDC as AD 435 678.)

5. Hogge, John E.: Three Ballistic Camera Data Reduction Methods Applicable to Reentry Experiments. NASA TN D-4260, 1967.

6. Lloyd, K. H.: Concise Method for Photogrammetry of Objects in the Sky. WRE-TN-72, Aust. Def. Sci. Serv., Aug. 1971.

7. Long, Sheila Ann Thibeault: Triangulation Error Analysis for the Barium Ion Cloud Experiment. M.S. Thesis, North Carolina State Univ., 1973.

8. Long, Sheila Ann T.: Derivation of Formulas for Root-Mean-Square Errors in Location, Orientation, and Shape in Triangulation Solution of an Elongated Object in Space. NASA TN D-7477, 1974.

9. Harp, Bill F.: Photogrammetric Calibration of the NASA-Wallops Island Image Intensifier System. Contract No. NAS 6-2066, DBA Systems, Inc., May 15, 1972. (Available as NASA CR-137455.)

10. Cain, Joseph C.; Hendricks, Shirley J.; Langel, Robert A.; and Hudson, William V.: A Proposed Model for the International Geomagnetic Reference Field-1965. J. Geomag. & Geoelec., vol. 19, no. 4, 1967, pp. 335-355.

11. Long, Sheila Ann T.: Analytical Expressions for Position Error in Triangulation Solution of Point in Space for Several Station Configurations. NASA TN D-7552, 1974.

TABLE I.- OBSERVATION STATIONS AND THEIR RESPECTIVE COORDINATES

Station	Geodetic latitude, deg	East longitude, deg	Altitude, km
Arequipa, Peru	-16.4667	-71.5000	2.4567
Cerro Tololo, Chile	-30.1667	-70.8167	2.1946
Mt. Hopkins, Arizona	31.6853	-110.8774	2.3640
NASA aircraft*	37.9324	-75.4717	10.6680
White Sands, New Mexico	32.4238	-106.5528	1.6500

*The NASA aircraft is assumed to be flying at an altitude of 10.7 km over Wallops Island, Virginia.

TABLE II.- AVERAGE POINTING DISPLACEMENT ERRORS FOR CASE 1 (FIVE STATIONS)

Spacing of input data points, deg	Average pointing displacement errors, km			
	East-west	North-south	Radial	Total
0.28	3	18	35	41
0.56	3	18	35	41
1.12	3	18	35	41
2.24	3	19	35	41
4.48	3	22	38	46
8.96	5	92	114	156

TABLE III.- STATION DISPLACEMENT ERRORS FOR FIVE-STATION CASE

Geocentric latitude, deg	Station displacement errors, km			
	East-west	North-south	Radial	Total
-9	4	3	37	37
0	4	13	31	34
9	4	16	21	26
19	3	12	11	17
28	3	8	5	10

TABLE IV.- STATION DISPLACEMENT ERRORS FOR FIVE-STATION CASE WITH INCORPORATION OF INPUT DATA FROM ONE ADDITIONAL CAMERA AT MT. HOPKINS

Geocentric latitude, deg	Station displacement errors, km			
	East-west	North-south	Radial	Total
-9	4	4	40	40
0	4	14	33	36
9	4	16	22	28
19	3	13	11	17
28	3	9	5	10

TABLE V.- STATION DISPLACEMENT ERRORS FOR FIVE-STATION CASE WITH INCORPORATION OF INPUT DATA FROM TWO ADDITIONAL CAMERAS AT MT. HOPKINS

Geocentric latitude, deg	Station displacement errors, km			
	East-west	North-south	Radial	Total
-9	4	4	41	41
0	4	14	34	37
9	4	17	22	28
19	3	13	11	17
28	3	9	5	11

L-74-8546

Figure 1.- Barium ion cloud as seen from Mt. Hopkins, Arizona, on September 21, 1971, at $3^h11^m14^s$ u.t. (The scale is at release altitude.)

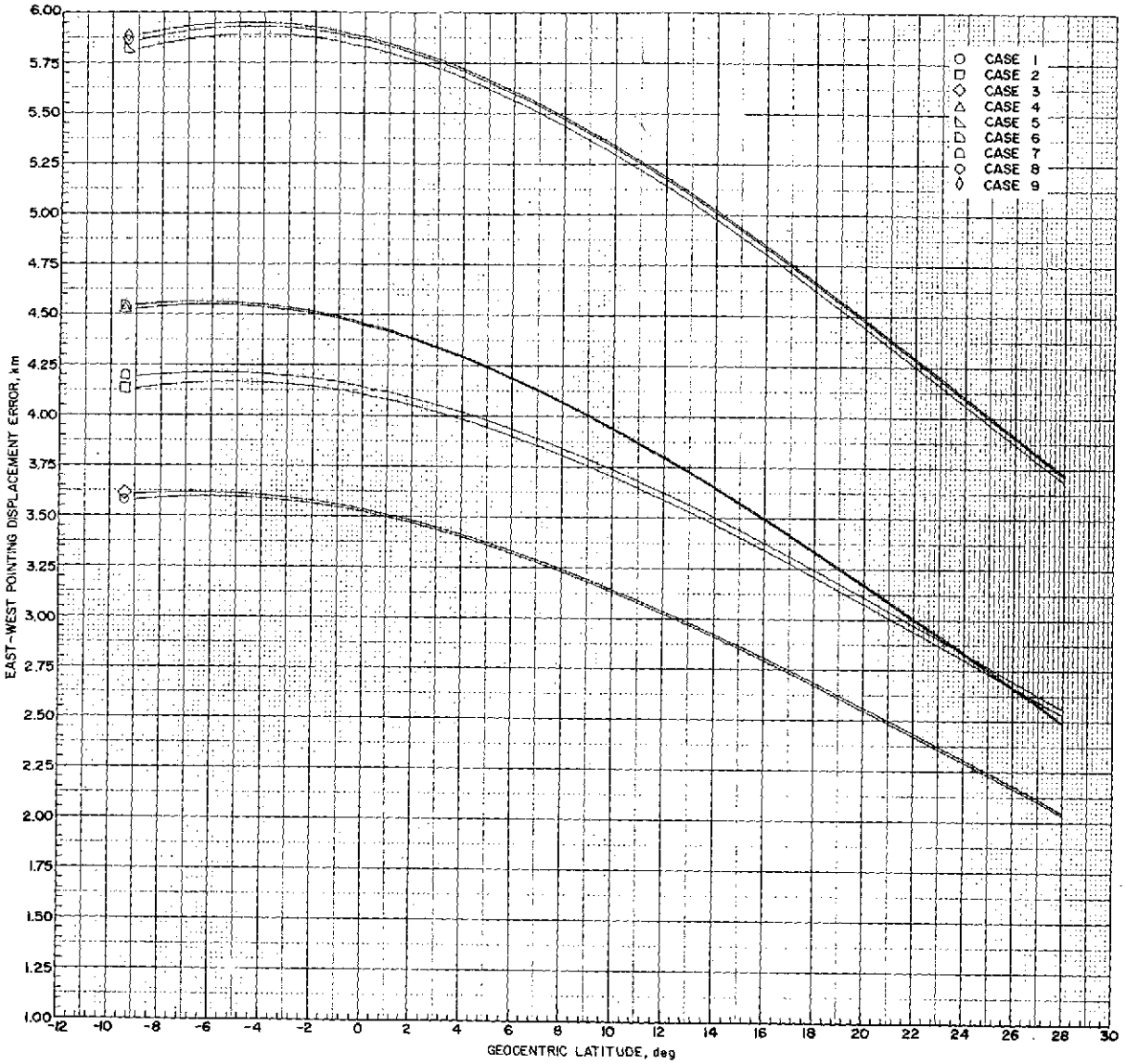

Figure 2.- East-west pointing displacement error for all station cases.

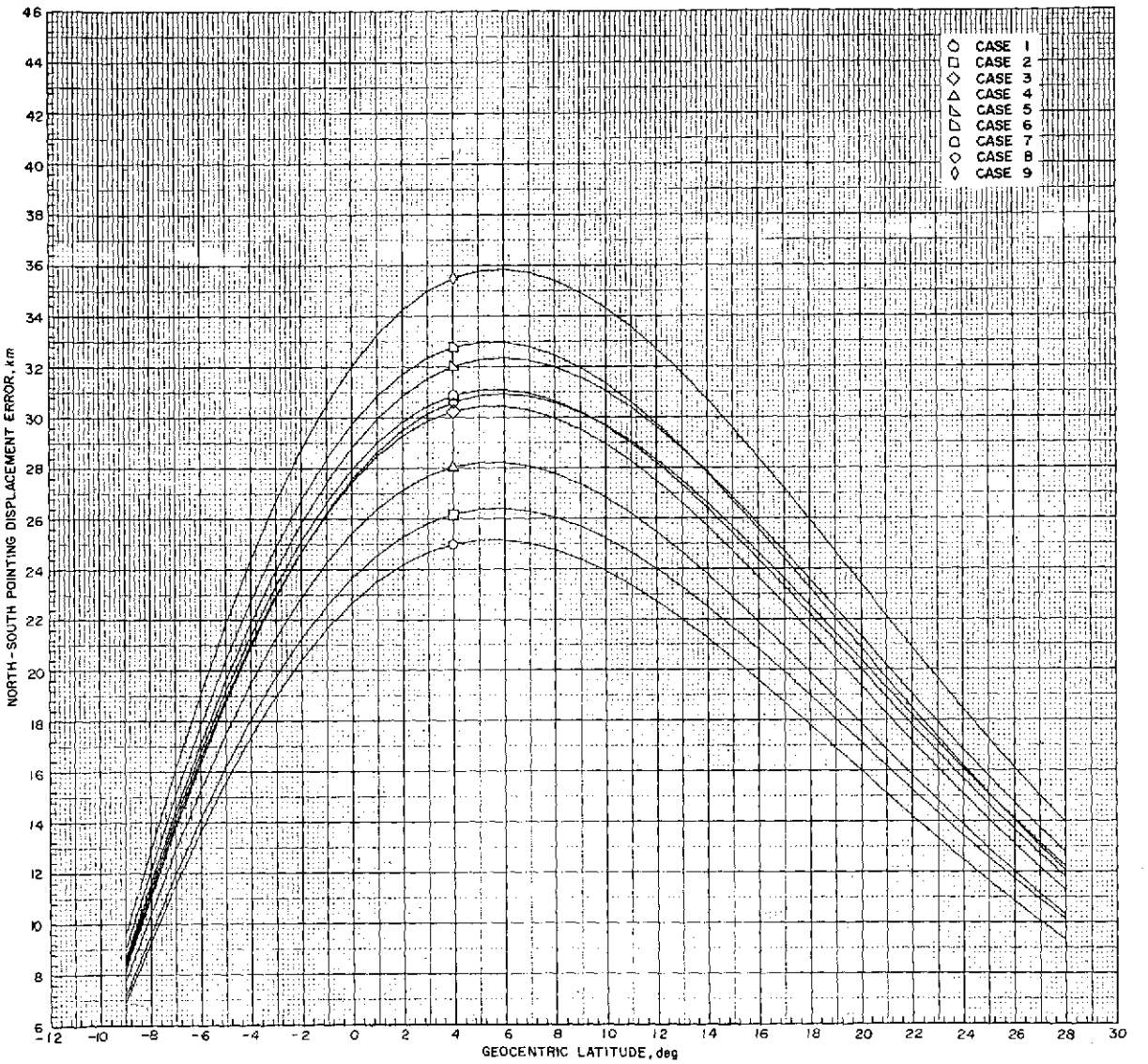

Figure 3.- North-south pointing displacement error for all station cases.

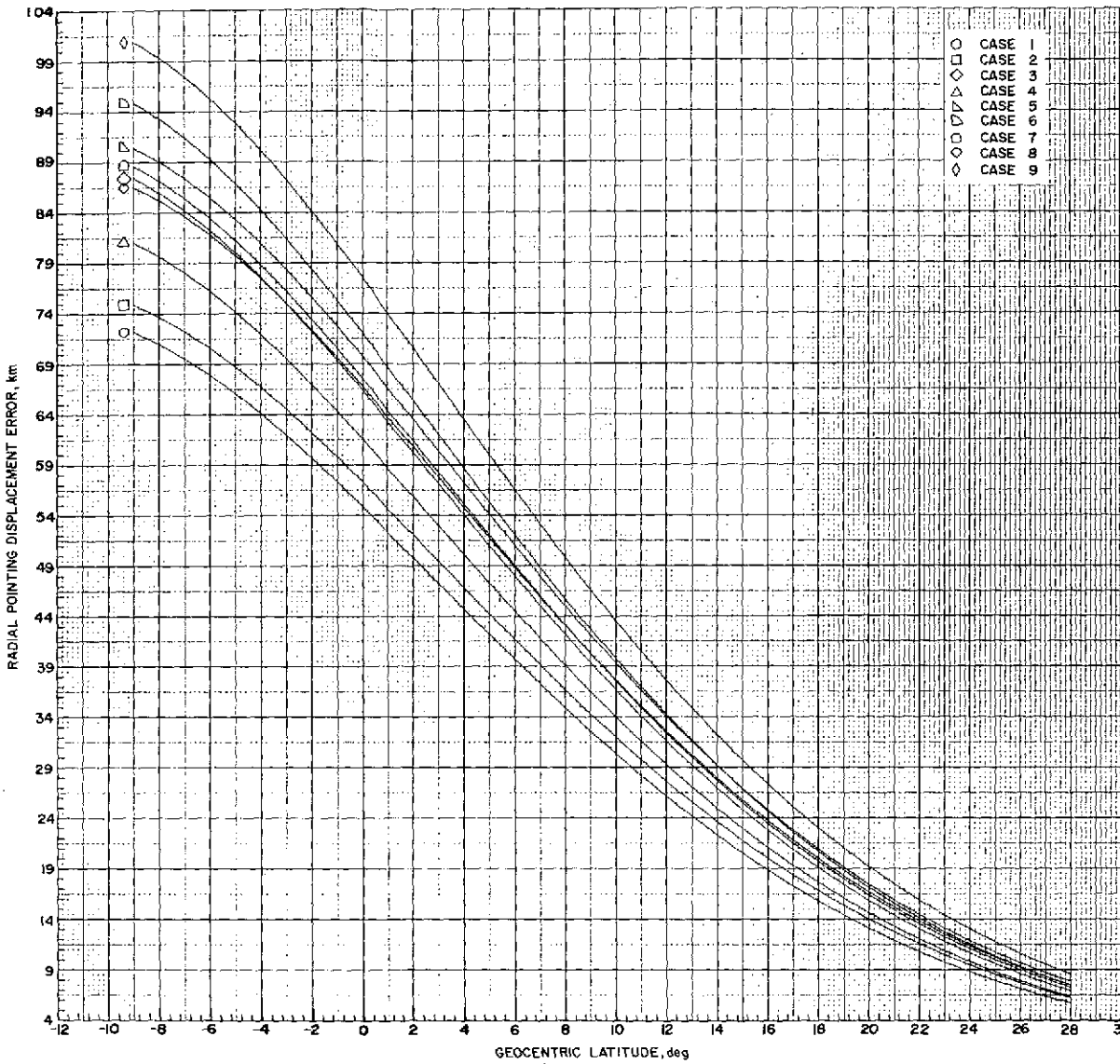

Figure 4.- Radial pointing displacement error for all station cases.

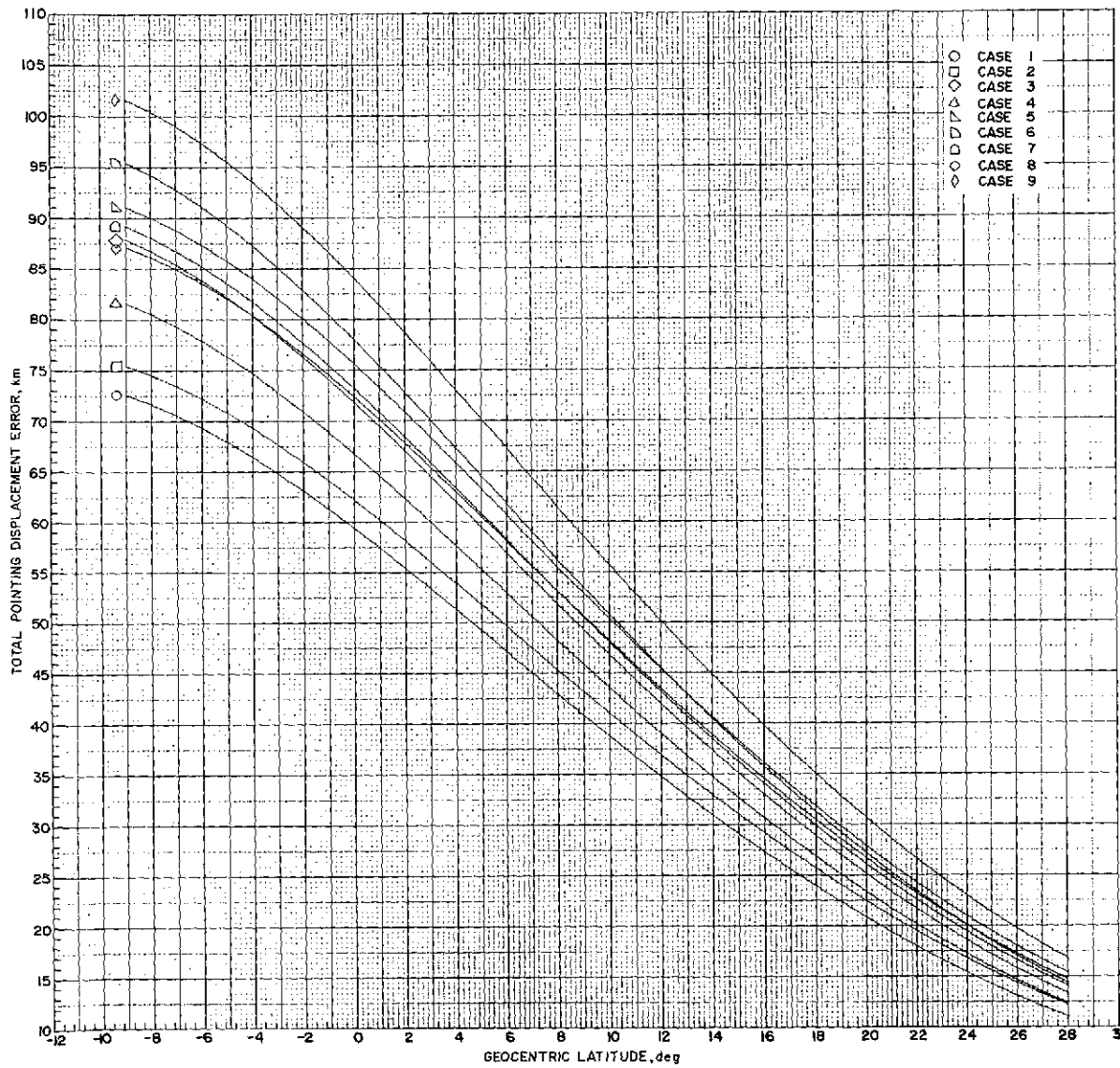

Figure 5.- Total pointing displacement error for all station cases.

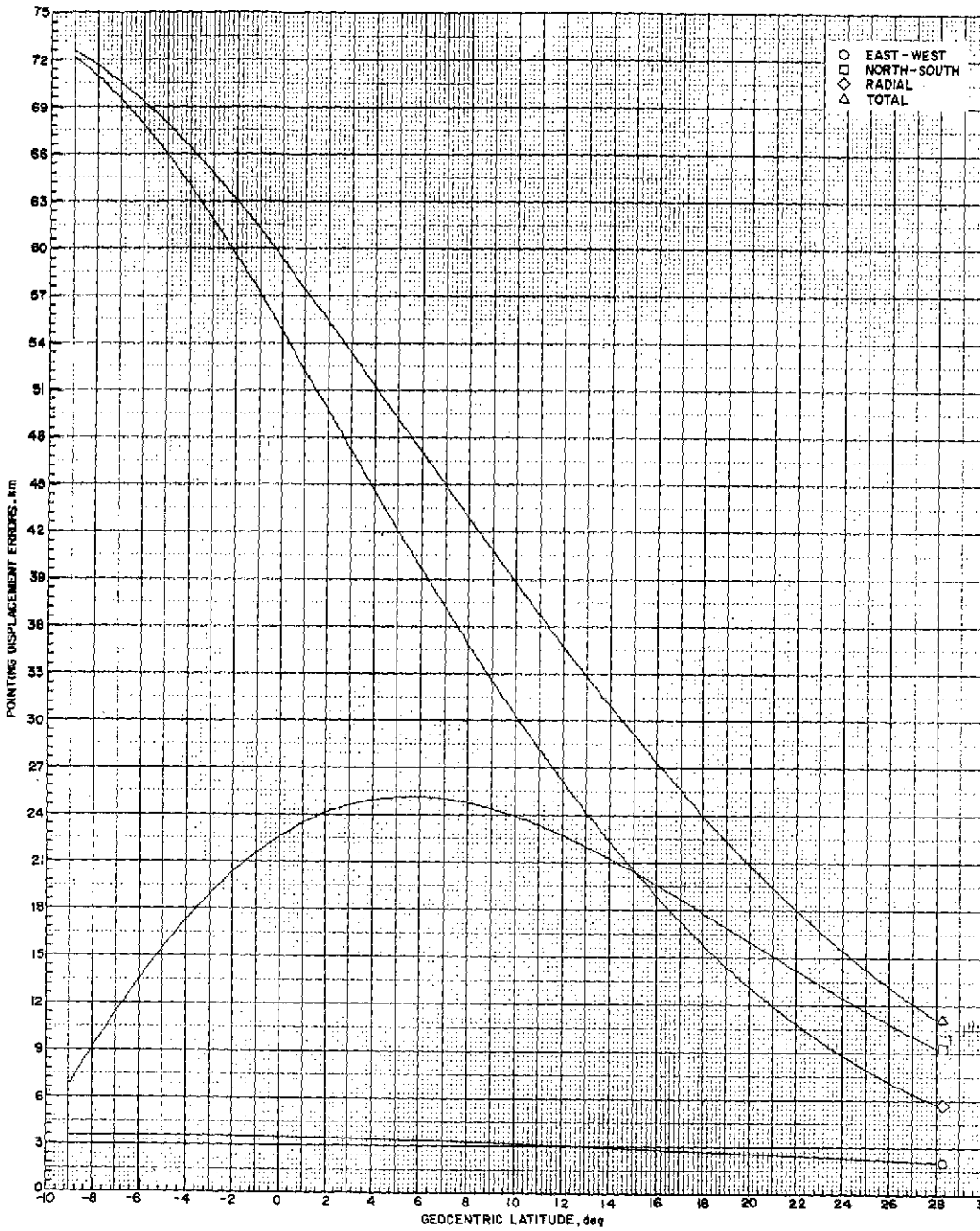

Figure 6.- Pointing displacement errors for case 1 (five stations).

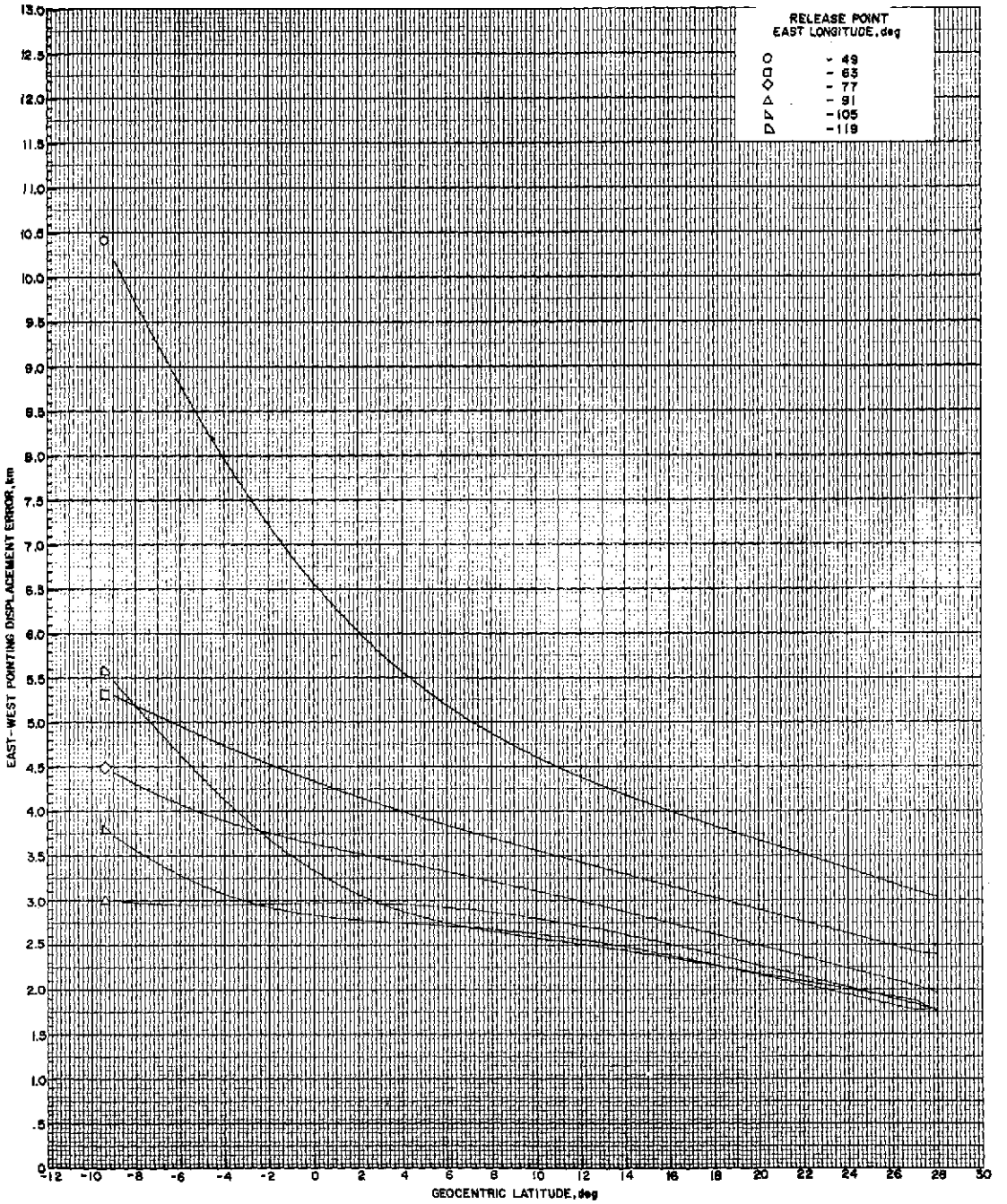

Figure 7.- East-west pointing displacement error for case 1 (five stations) for release points varying in east longitude.

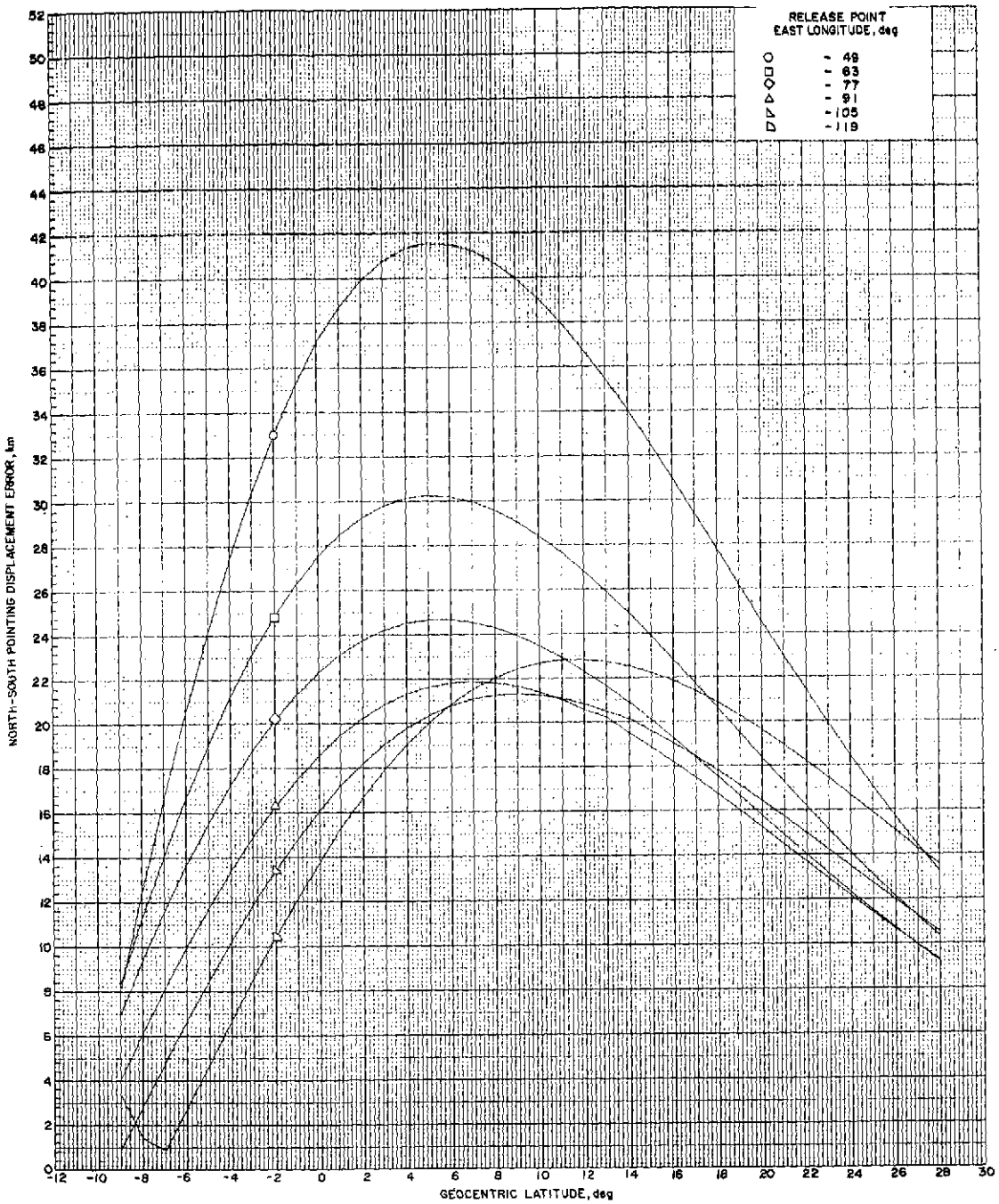

Figure 8.- North-south pointing displacement error for case 1 (five stations) for release points varying in east longitude.

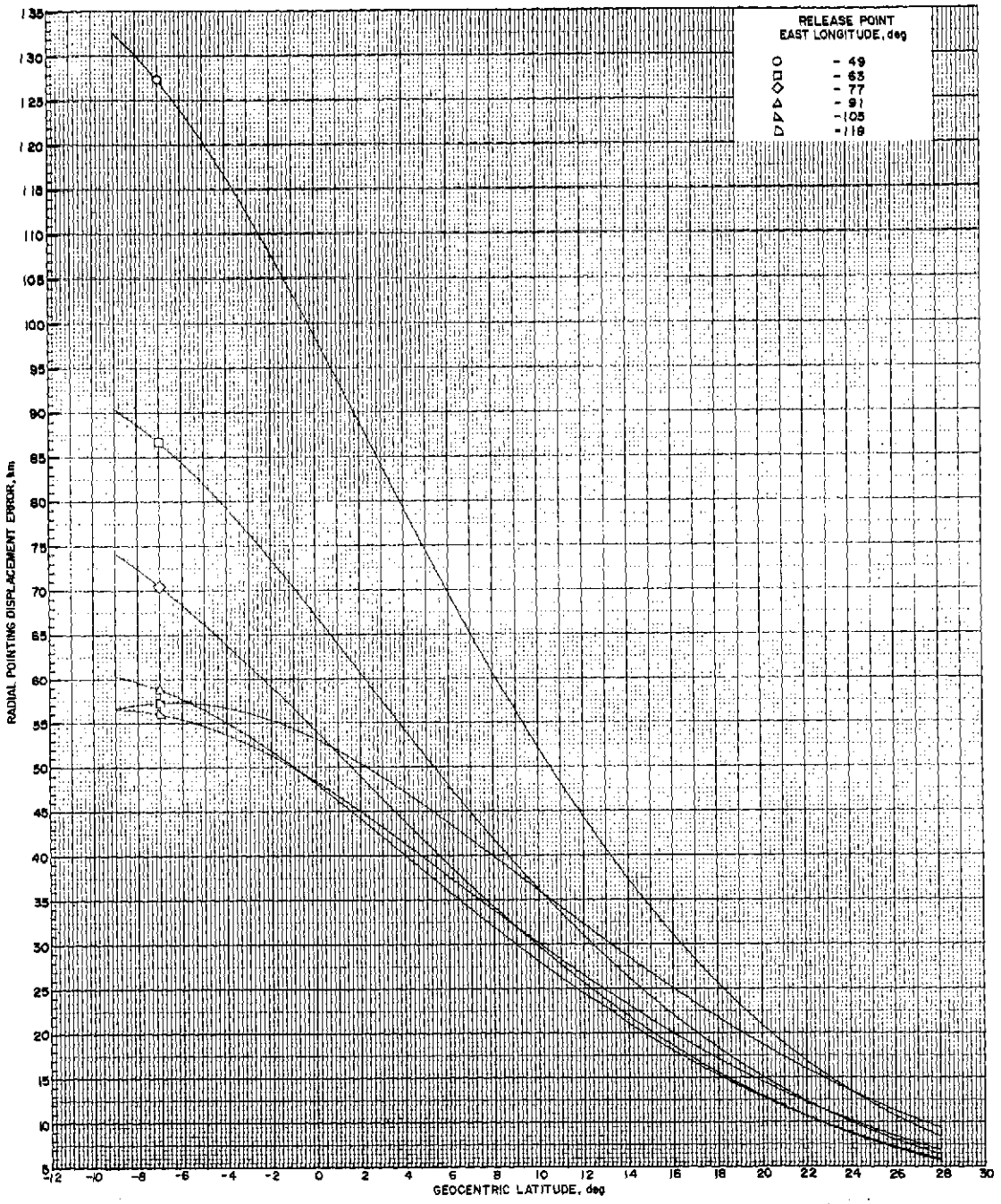

Figure 9.- Radial pointing displacement error for case 1 (five stations) for release points varying in east longitude.

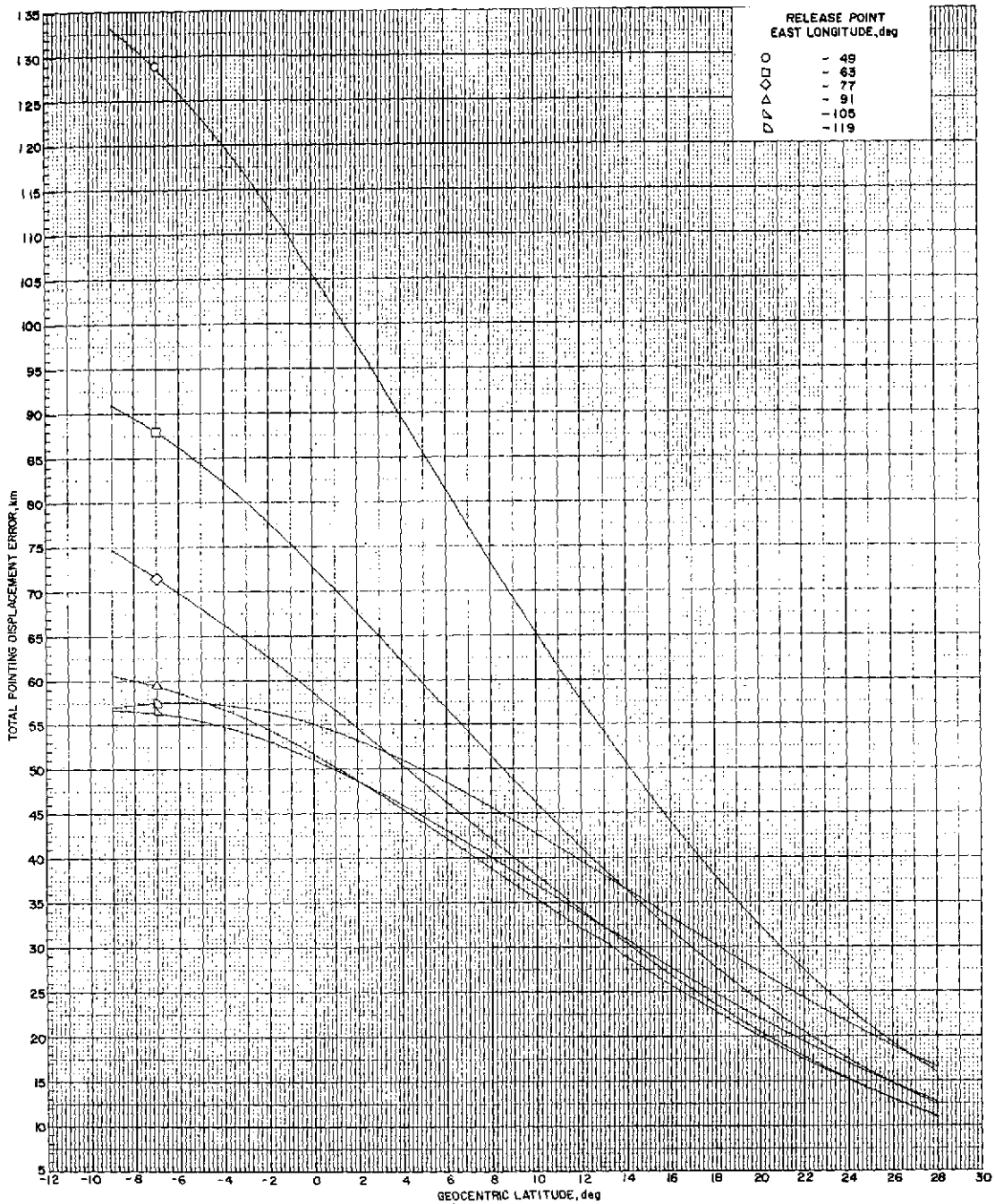

Figure 10.- Total pointing displacement error for case 1 (five stations) for release points varying in east longitude.

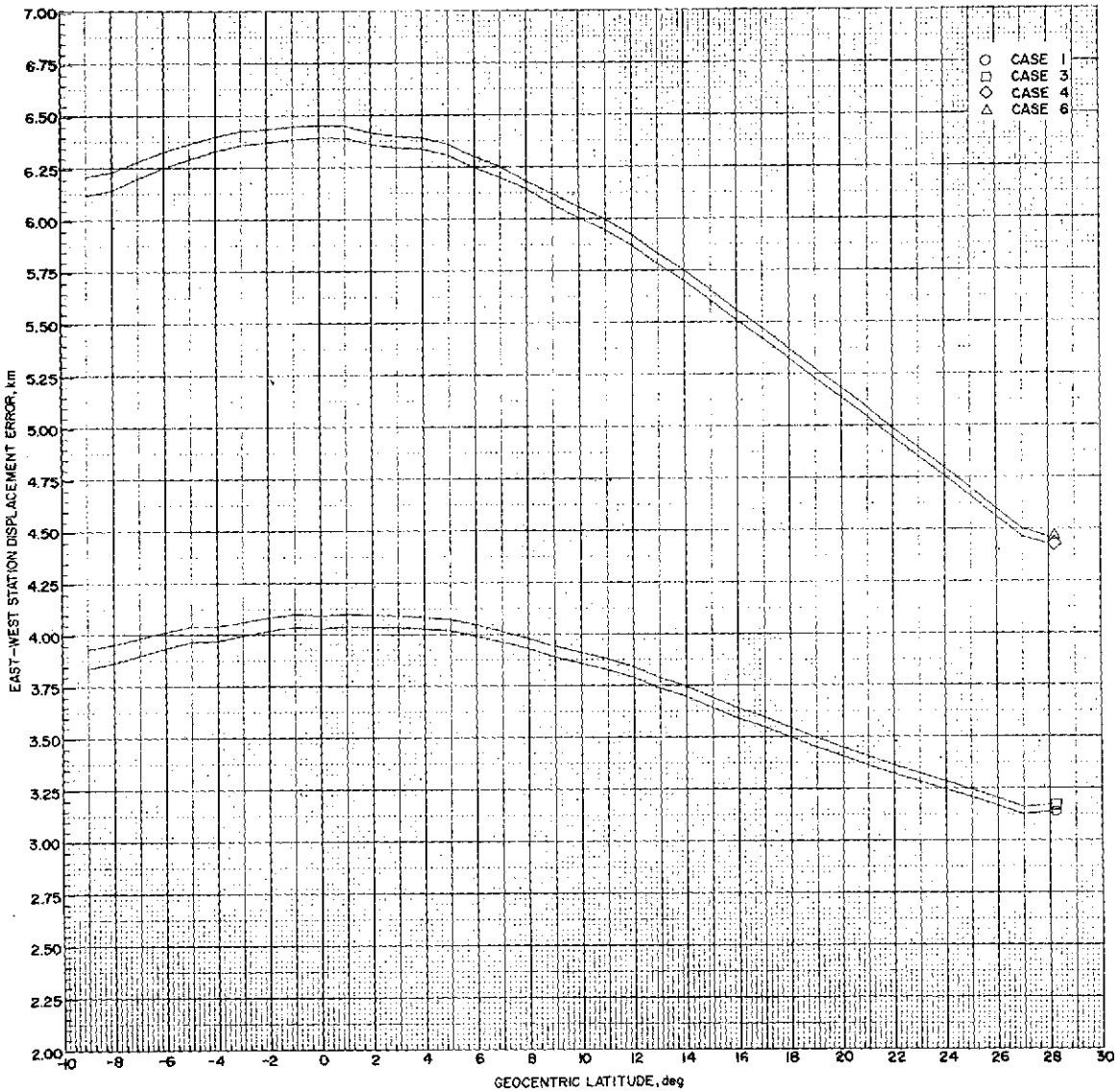

Figure 11.- East-west station displacement error for station cases that include NASA aircraft.

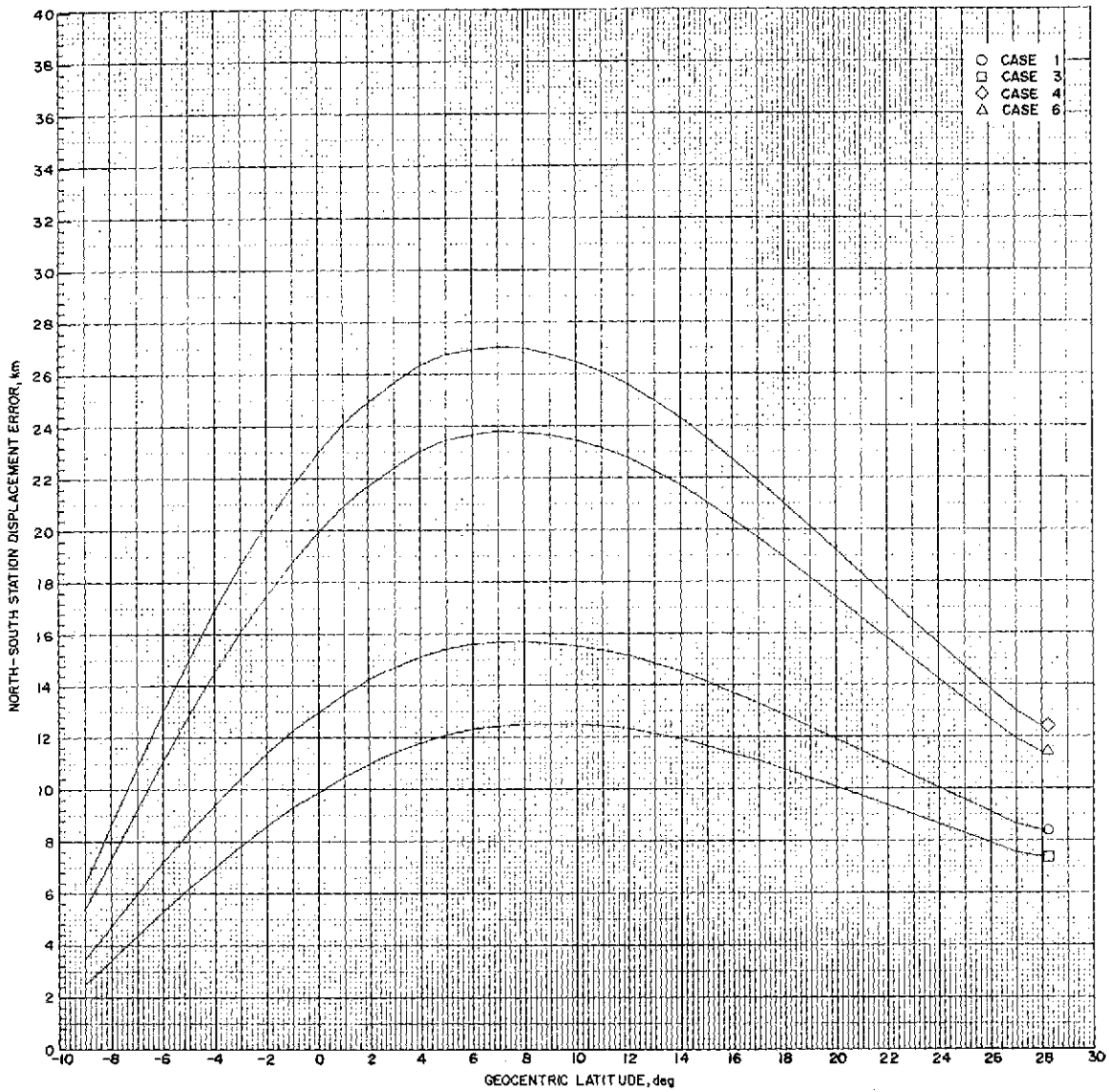

Figure 12.- North-south station displacement error for station cases that include NASA aircraft.

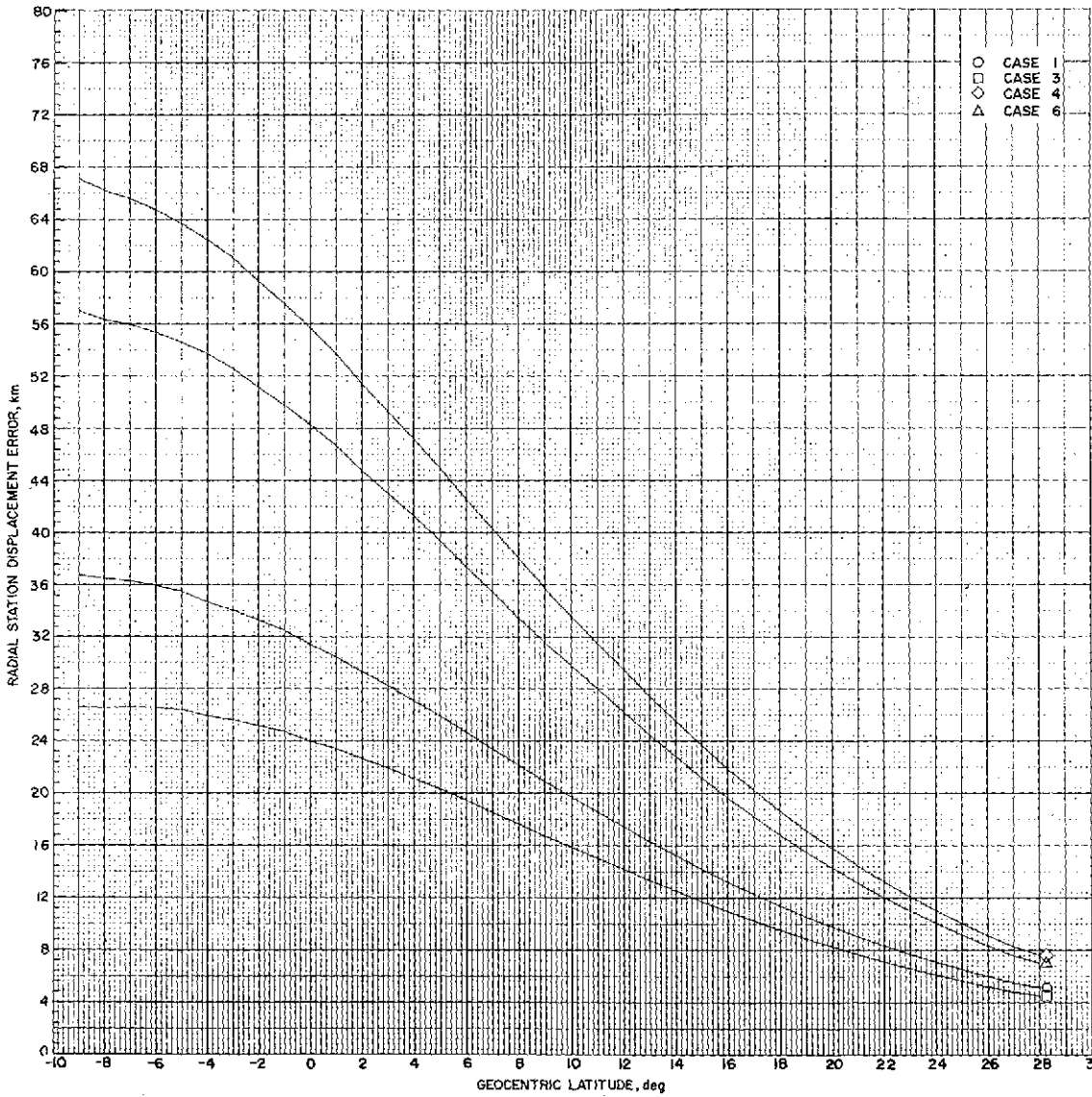

Figure 13.- Radial station displacement error for station cases that include NASA aircraft.

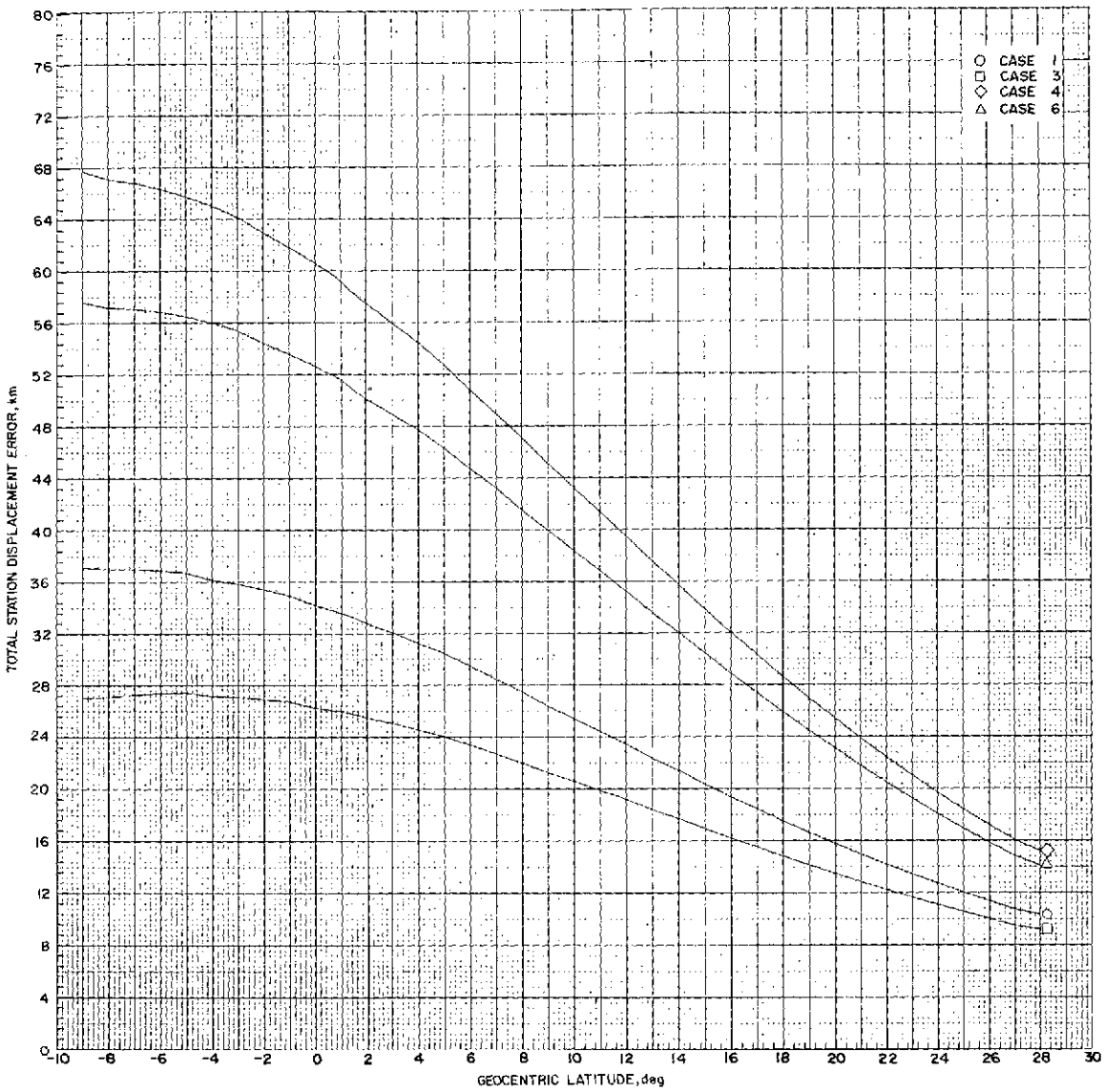

Figure 14.- Total station displacement error for station cases that include NASA aircraft.